Narrow Lines in Type II Supernovae – Probing the Circumstellar Nebulae of the Progenitors

Robert A. Gruendl, You-Hua Chu[1,2]

Astronomy Department, University of Illinois, 1002 West Green Street, Urbana, IL 61801

gruendl@astro.uiuc.edu, chu@astro.uiuc.edu

Schuyler D. Van Dyk[1]

IPAC/Caltech, Mail Code 100-22, Pasadena, CA 91125

vandyk@ipac.caltech.edu

Christopher J. Stockdale[3]

Department of Physics and Astronomy, University of Oklahoma, 440 West Brooks, Room 131, Norman, OK 73019

stockdal@rsd.nrl.navy.mil

ABSTRACT

We have carried out a high-dispersion (R∼30,000) echelle spectroscopic survey of 16 Type II supernovae (SNe) to search for narrow emission lines from circumstellar nebulae ejected by their massive progenitors. Circumstellar nebulae, if detected, provide invaluable opportunities to probe SN progenitors. Of the 16 SNe observed, SN ejecta are clearly detected in 4 SNe and possibly in another 2 SNe, interstellar gas is detected in 12 SNe, and circumstellar material is detected only in SN 1978K and SN 1998S. In the case of SN 1978K we are able to place an upper limit of ∼2.2 pc for the size of the circumstellar ejecta nebula and note that this is more consistent with the typical sizes observed for ejecta nebulae around luminous blue variables rather than Wolf-Rayet stars. In the case of SN 1998S, our observations of the narrow lines ∼1 year after the SN explosion show variations compared to early epochs. The nebular lines we observe from SN 1998S originate from either the low–density, outer region of a circumstellar nebula or have become dominated by an interstellar component.

Subject headings: supernovae – circumstellar matter — ISM: bubbles

[1]Visiting astronomer, Kitt Peak National Observatory

[2]Visiting astronomer, Cerro Tololo Inter-American Observatory

[3]Current address: Naval Research Laboratory, NRL-Code 7213, Washington, DC 20375

1. Introduction

Supernovae (SNe) of Types Ib, Ic, and II are believed to have massive progenitors, because they have been found frequently in or near spiral arms and H II regions but not in elliptical galaxies (Van Dyk, Hamuy, & Filippenko 1996). Few SNe (e.g., SN 1987A) have recognized massive progenitors; consequently, little is known about the stellar evolution immediately before the SN explosion.

Evolved massive stars are known to undergo copious mass loss, forming circumstellar nebulae. The rings around SN 1987A are an example of such a nebula (Burrows et al. 1995). The chemical composition and kinematics of the rings have provided essential constraints that lead to the hypothesis that the B3I progenitor Sk $-69°202$ was a binary (Podsiadlowski 1992). These circumstellar nebulae can also be detected from the presence of narrow Hα emission lines (FWHM $\leq$ 200 km s^{-1}) in spectra of Type IIn SNe (Schlegel 1990; Filippenko 1991, 1997). The circumstellar nebulae of distant SNe cannot be resolved spatially, but their expansion, physical conditions, and chemical enrichment can be investigated by high-dispersion (R $\geq$ 30,000) spectra, as recently demonstrated for SN 1997ab (Salamanca et al. 1998) and SN 1978K (Chu et al. 1999).

Most available spectroscopic observations of SNe have been made with low or intermediate spectral dispersion to study the broad spectral lines of SN ejecta. These spectra are useful for revealing the presence of narrow nebular lines, but are not adequate for analysis of nebular kinematics and physical conditions. Therefore, we have undertaken a high-dispersion spectroscopic survey of 16 Type II SNe. The results are reported in this paper.

2. Observations

High-dispersion spectra were acquired with the echelle spectrograph using the Kitt Peak National Observatory (KPNO) 4m telescope in March 1999. The 79 line mm^{-1} echelle grating was used in combination with a 226 line mm^{-1} cross-disperser and the long-focus red camera to achieve a reciprocal dispersion of 3.5 Å mm^{-1} at Hα. The spectra were imaged with the T2KB CCD detector, where the pixel size of 24 μm corresponds to $0\farcs24$ pixel^{-1} along the slit and $\sim$3.7 km s^{-1} pixel^{-1} at the Hα line along the dispersion axis. The spectral coverage was roughly 4000–7000 Å. The instrumental resolution for the $1''$ wide slit, as measured from the widths of sky lines, was $\sim$10 km s^{-1}(FWHM) at Hα.

The sky conditions were moderate to poor due to variable high cirrus and nearly full lunar phase, making the target acquisition difficult at times. The spectra were reduced using the echelle and longslit packages in IRAF with careful attention paid to the orders that contained Hα emission. Observations of the spectrophotometric standard GD 140 were used to correct for the blaze, illumination, and spectral response, but the resulting spectra were not calibrated to an absolute flux scale as the observing conditions were not photometric.

In addition to the objects observed at KPNO, we have also observed SN 1978K with the

echelle spectrograph on the 4m telescope at the Cerro Tololo Inter-American Observatory (CTIO) in December 2000. The instrument was configured with similar optical elements as were used for the KPNO observations, and the spatial and spectral parameters are therefore similar. All observations are summarized in Table 1.

3. Results

Our high-dispersion echelle observations are useful in distinguishing among three sources of line emission in distant SNe:

- SN ejecta, which can be identified by a broad (width > 1000 km s^{-1}), spatially-unresolved Hα line;
- Unshocked circumstellar material (CSM) ejected by the SN progenitor, which shows narrow (width ≤ 200 km s^{-1}), spatially-unresolved Hα and [N II] $\lambda\lambda$6548, 6583 lines; and
- Interstellar medium (ISM) of the host galaxy, which is characterized by narrow, spatially-extended Hα emission and forbidden lines such as [O III] λ5007 and [S II] $\lambda\lambda$6716,6731.

To search for emission from the SN, CSM, and ISM in each of our spectra, we used the spatio-kinematic descriptions of line emission given above along with the criterion that the statistical significance of the peak of an emission component be $>3\sigma$ per resolution element (e.g., $\sim$10 km s$^{-1}\times$ 1$''$ at Hα) with respect to the background rms noise. The results are summarized in Table 2.

Of the 16 SNe observed, we clearly detect broad line emission from the SN ejecta from four sources: SN 1978K, SN 1995N, SN 1997eg, and SN 1998S. In two further cases, SN 1999E and SN 1999Z, broad Hα emission line may be detected, but significant portions of the line profiles are lost between echelle orders. It is difficult to distinguish between the line and continuum emission components from the SN ejecta of these two latter objects.

Our low detection rate of the SNe is likely caused by the faintness of the SNe and the poor sky condition. The majority of the SNe observed were not visible in the images taken by the acquisition camera. Blind offsets from nearby stars had to be employed for target acquisition. If the coordinates of a SN from the literature were off by more than 1$''$ perpendicular to the slit, our blind-offset observations would have missed the target entirely.

The Hα echellograms and line profiles of SN 1995N, SN 1997eg, SN 1998S, SN 1999E, and SN 1999Z are presented in Figure 1a&b, along with finding charts. Spectral scales are given in both observed wavelengths and velocities relative to the host galaxy's systemic velocity. The broad Hα emission from the SN ejecta, detected over several thousand km s^{-1}, is evident in each image.

SN 1978K was detected with the highest signal-to-noise (S/N) ratio; several lines were detected. Its Hα line image and the profiles of 10 spectral lines are presented in Figure 2. While Hα, Hβ, and He I λ5876 lines of the SN ejecta are broad, they are not as broad as the Hα line of the

other three SNe we detected. More interestingly, a narrow nebular component is detected in Hα, [N II] $\lambda\lambda$6548, 6583 and [O III] λ5007 lines. The high [N II]/Hα ratio indicates that this narrow component originates from a circumstellar nebula (Chu et al. 1999).

Besides SN 1978K, the only other SN in our sample that shows emission components from a circumstellar nebula is SN 1998S. In Figure 3 we show the narrow Hα, [N II], and [O III] components detected in this spectrum. The identification of a circumstellar component in SN 1998S is not as straightforward as that for SN 1978K because of the presence of a bright interstellar component. Details of this identification are given in §3.5 below.

Extended interstellar emission is detected in our observations of 12 SNe. This high detection rate (12 out of 16) is fully consistent with their being Type II SNe with massive progenitors. Three examples of interstellar Hα emission are presented in Figure 4. The interstellar Hα line, compared to the telluric OH and Hα lines, is broader and shows velocity variations along the slit.

In the remainder of this section we summarize the observed properties of individual objects that are interesting.

3.1. SN 1954J and SN 1961V

SN 1954J and SN 1961V, in NGC 2403 and NGC 1058 respectively, had spectral properties similar to a Type II SN, but were peculiar in four respects: 1) the linewidths of SN 1961V correspond to an expansion velocity of only 2000 km s^{-1}, 2) the progenitors were known, 3) they were underluminous, and 4) their SN light curves were followed in the optical for up to eight years. It has been suggested that SN 1954J and SN 1961V are luminous blue variables (LBVs) similar to η Car (Humphreys & Davidson 1994; Goodrich et al. 1989).

In optical and near-infrared imaging observations more recent than our echelle observations, Smith, Humphreys, & Gehrz (2001) have identified a faint red star with a position consistent with V12, the progenitor of SN 1954J. Similarly, using *Hubble Space Telescope* (*HST*) WFPC1 images of SN 1961V, Filippenko et al. (1995) have tentatively identified a faint red star with a position consistent with SN 1961V. In either case, these red sources could be a post-eruption LBV, but neither observation can rule out that these sources are an unrelated red supergiant. Spectroscopic observations similar to those reported in this paper are needed. Our observations of SN 1954J and SN 1961V were based on the best coordinates for the SNe that were available. While no emission from a SN or a post eruption LBV are detected in these spectra, interstellar emission red-shifted by $\sim$ 20 km s^{-1} with respect to the systemic velocity of each host galaxy are present in the spectra. The coordinates of the candidate post-eruption LBV tentatively associated with SN 1954J (Smith et al. 2001) place it more than 2″ from our 1″ echelle slit center and therefore our observations do not include significant emission from this source.

Optical Hα+[N II], [O III], and [S II] images of the vicinity of SN 1961V show two H II

regions separated by $\sim 3''$ (Fesen 1985) that are coincident with two non-thermal radio sources (Branch & Cowan 1985; Cowan, Henry, & Branch 1988). The eastern source is roughly coincident with SN 1961V. Recent VLA observations at 6 cm and 18 cm by Stockdale et al. (2001) confirm that both radio sources are non-thermal and show that SN 1961V's radio emission has decayed. These observed properties are consistent with many known SNe that have been recovered at radio wavelengths.

Our observations of SN 1961V show two narrow-line ($\sim$30 km s^{-1}) sources in Hα and [O III] that are coincident with the two H II regions, but no broad Hα emission line is detected in 2 hrs of integration time. Furthermore, we do not detect [N II] emission that might be expected if nitrogen enriched material in an LBV ejecta nebula is present. It is possible that our slit just missed SN 1961V. As shown in Figure 5, the two radio sources are not exactly coincident with the two H II regions. The eastern radio source, corresponding to SN 1961V and coincident with the LBV candidate identified by Filippenko et al. (1995), is $\sim 2''$ southwest of the core of the eastern H II region. Since our E-W echelle slit was centered on the two H II regions, whose central star clusters were the only objects visible in the telescope acquisition image, the $1''$ slit width could have easily missed SN 1961V and the LBV candidate.

3.2. SN 1978K

A host of lines are detected from SN 1978K in NGC 1313 (see Figure 2). We clearly detect broad Hα, Hβ, and He I λ5876 emission lines. Furthermore, we have a tentative weak detection of broad [O I] λ6363 emission. Note that the stronger [O I] λ6300 was not detected because it has been Doppler shifted into a gap between echelle orders. In addition to broad emission lines, we detect narrow, spatially unresolved, emission from He II λ4686, [O III] $\lambda\lambda$ 4959,5007, [N II] λ5755, and [N II] $\lambda\lambda$6548,6583. Interestingly, the [S II] $\lambda\lambda$6716,6731 lines are not detected. The implications of the line detections and non-detections from SN 1978K will be discussed further in § 4.

3.3. SN 1995N

We detect broad Hα emission from SN 1995N (see Figure 1a), with FWZI (full-width at zero intensity) of $\sim$3,000 km s^{-1}. In addition, a narrow interstellar component with FWHM $\sim$30 km s^{-1} is present. While the interstellar emission is red-shifted by roughly 40 km s^{-1} from the the systemic velocity of the host galaxy Arp 261, the broad Hα emission appears to be blue-shifted by $\sim$200 km s^{-1}.

3.4. SN 1997eg

Our observations of SN 1997eg detect broad Hα emission with FWZI of $\sim$3,500 km s^{-1} which is blue-shifted by $\sim$400 km s^{-1} with respect to the host galaxy NGC 5012. Furthermore, these observations show narrow Hα and [N II] λ6583 emission components and possibly narrow [S II] $\lambda\lambda$6716,6731 emission blue-shifted by $\sim$160 km s^{-1} with respect to the systemic velocity of the host galaxy. The Hα and [N II] emission are both narrow and are clearly visible throughout the echelle slit and therefore are interstellar in origin. Salamanca, Terlevich, & Tenorio-Tagle (2002) observed SN 1997eg $\sim$1 yr earlier and detected a strong, narrow, P-Cygni profile caused by CSM, which has completely vanished at the time of our observations.

3.5. SN 1998S

The Hα spectrum of SN 1998S in NGC 3877 shows a total width greater than 10,000 km s^{-1}. Superposed on this broad component from the SN ejecta, we find a narrow Hα feature at $\sim$6581 Å extending along the slit across the SN. The spatial distribution indicates the presence of ISM in the vicinity of SN 1998S. In addition we detect narrow, spatially extended, [N II] λ6583 and narrow, spatially unresolved [O III] $\lambda\lambda$4959,5007 emission (see Figure 3). Comparison between the Hα and [N II] lines on and off the SN position does not show conclusively the existence of a circumstellar nebula. The presence of the spatially unresolved [O III] emission indicates that there is a nebula associated with the SN progenitor. The heliocentric velocities of the narrow Hα, [N II], and [O III] lines extracted at the position of the SN are -66, -74, and -64 km s^{-1}, respectively, relative to the systemic velocity of the NGC 3877. The velocity difference between the [N II] line and the other two lines are larger than the uncertainty of the measurements, $\sim$3 km s^{-1}, indicating that these narrow components may have a complex origin consisting of an unknown mixture of CSM and ISM.

We can further compare our observations of SN 1998S, taken $\sim$1 year after its discovery, to the high dispersion spectra taken 17.4 and 36.3 days after the discovery (Fassia et al. 2001). Only the [O III] λ5007 line shows continuity from one epoch to the next. The line shape changes from an asymmetric profile on day 17.4, to a broader (FWHM=59$\pm$9 km s^{-1}) and symmetric profile on day 36.3, to a narrower (FWHM=37$\pm$3 km s^{-1}) symmetric profile centered at the same velocity 1 year later. At Hα, the early nebular line had a P-Cygni profile, while our spectra show the line only in emission. The most dramatic difference between the early observations and our observations is in the [N II] lines. The [N II] lines were not detected on day 17.4; the auroral [N II] λ5755 line was observed to be at least 3 times as strong as the nebular [N II] λ6583 line on day 36.3; 1 year later, the nebular [N II] line was detected but the auroral [N II] line was not detected.

The early line ratios indicate the presence of ionized gas denser than 10^6 cm^{-3} which can only be circumstellar in origin (Fassia et al. 2001). If the narrow nebular features from all three epochs originate from the same nebula, then our observations detect the outer, low–density region of this circumstellar nebula. On the other hand, we cannot rule out the possibility that the narrow,

spatially unresolved spectral features we observed have a significant contribution from the ISM.

3.6. SN 1998bm

The galactic environment of SN 1998bm is complex and it remains unclear whether it is in NGC 2820 or NGC 2820A. SN 1998bm itself is not detected, but the interstellar emission in the echellogram appears consistent with that of an expanding shell of size ∼600 pc. While this interstellar emission might be from a supergiant shell, the expansion velocity, ∼75 km s^{-1}, is relatively high compared to similar resolved structures in the Large Magellanic Cloud (Points et al. 1999) and other galaxies (Hunter & Gallagher 1997). We therefore conclude that the emission lines detected are likely a superposition of the ISM of both NGC 2820 and NGC 2820A. Each of these interstellar emission components is blue-shifted with respect to the systemic velocity of the two galaxies. The brighter component (toward the western end of the slit) is probably associated with NGC 2820A and is blue-shifted by ∼80 km s^{-1}. It is less certain from which galaxy the fainter component might arise but it is blue-shifted by either ∼120 km s^{-1} or ∼160 km s^{-1} from the systemic velocity of NGC 2820 and NGC 2820A, respectively.

3.7. SN 1999E

Our observation of SN 1999E detects faint, spatially-unresolved, broad emission features throughout the entire echellogram. The high dispersion of the spectrum and the gaps between echelle orders make it difficult to identify these emission features. It is nevertheless clear that these emission features are unlike that of any stars; therefore, we believe that the broad emission features are from the young SN 1999E. In addition to the broad features, narrow interstellar Hα, Hβ, and [O III] λ5007 emission are detected. The Hα emission detected has an average heliocentric velocity of 7,925±10 km s^{-1} and FWHM of ∼100 km s^{-1}. Both the Hβ and [O III] lines have similar redshifts and all lines have a velocity 185 km s^{-1} greater than the previously reported systemic velocity of the host galaxy IRAS 13145−1817 (Nicolaci da Costa et al. 1998).

3.8. SN 1999Z

Our observation of SN 1999Z also detects faint, spatially-unresolved, broad emission features throughout the entire echellogram. Similarly, we believe that these emission features originate from SN 1999Z. The Hα line is red-shifted into a gap between echelle orders but narrow interstellar components of Hβ, [O III] λ5007, and [S II] $\lambda\lambda$6716,6731 are detected. Based on the two strongest lines, Hβ and [S II] λ6716, we find a heliocentric velocity of 15,450±10 km s^{-1} for the emission lines which is ∼350 km s^{-1} greater than that previously reported for UGC 05608 by Jha et al. (1999) which were based on the apparent velocity centroid of the then newly detected SN line emission.

4. Discussion

The very last evolutionary stage of a massive star before SN explosion is not well known. It is impossible to study SN progenitors after they have exploded, but it is possible to study the CSM shed by the progenitors and photoionized by UV flashes from the SNe. The physical properties of these circumstellar nebulae may provide invaluable information about the doomed massive stars.

In the last hundred years, SN 1987A has been the only SN observed in the Local Group. All the other SNe are in distant galaxies, where circumstellar nebulae can only be detected in high-dispersion spectra of SNe as narrow nebular lines with high [N II]/Hα ratios. The size of an unresolved circumstellar nebula can be determined if the SN is spectroscopically monitored until the SN ejecta impact the circumstellar nebula. For example, if SN 1987A were at a large distance, the size of its inner ring nebula could still be determined from the 10–11 years time lapse from the SN explosion to the emergence of a broader nebular component, and the 15,000 km s^{-1} expansion velocity of the SN ejecta inferred from its broad Lyα emission (Michael et al. 2000).

There are apparently two types of circumstellar nebulae produced by SN progenitors. The first type of circumstellar nebulae are swept-up by SN ejecta within a year or two, as demonstrated dramatically in time-sequenced spectra for SN 1988Z (Stathakis & Sadler 1991). In the case of SN 1997eg, previous observations have shown a narrow P-Cygni component to the SN spectrum (Salamanca et al. 2002) which has disappeared at the time of our observations, one year later. These nebulae are small ($\sim$0.01 pc), and, for the case of SN 1997eg, very dense ($\geq 10^7$ cm^{-3}). Such ionized nebulae have not been observed around any known evolved massive stars. This circumstellar material may have been ejected immediately before the SN explosion (Chu 2001) or during a red supergiant phase (Fassia et al. 2001).

The second type of circumstellar nebulae are longer lived, indicating a larger size. These nebulae might be the counterparts of circumstellar nebulae observed around Wolf-Rayet (WR) stars or LBVs (Chu, Weis, & Garnett 1999). For a nebular radius of 2 pc and a SN ejecta expansion velocity of 10,000 km s^{-1}, the impact of SN ejecta on the circumstellar nebula is expected at $\sim$200 yr after the SN explosion, and the impact will produce X-ray-luminous SNRs such as the one observed in NGC 6946 (Dunne et al. 2000) and the SNR 0540$-$69.3 in the Large Magellanic Cloud (Caraveo, Mignani, & Bignami 1998).

Among the SNe we surveyed, we detect CSM around SN 1978K and SN 1998S. In the case of SN 1978K, the circumstellar nebula was not yet hit by the SN ejecta 21 years after the SN explosion. This must belong to the second type of circumstellar nebula described above. In the case of SN 1998S, the rapid temporal evolution of the spectral lines from the CSM over the first year indicate that this material is interacting with the SN ejecta and must belong to the first type.

Our new observations of SN 1978K confirm the Hα and [N II] line emission and expansion velocity of the CSM previously reported by Chu et al. (1999). As this circumstellar nebula is in the second class mentioned above and NGC 1313 is relatively nearby, the nebula might be large enough

to be resolved by the *HST*. Therefore, we obtained the *HST* archive WFPC2 images of SN 1978K taken with F656N and F606W filters on 1998 September 23 as part of program GO-6713 (PI: W. Sparks). In these observations the SN is centered in the PC and a point-like source is detected (see Figure 6). Also shown in Figure 6 are the expected point-spread-functions for position of the SN in the PC for observations with the F656N and F606W filters.[4] These images clearly place an upper limit of 0.″1 on the size of the circumstellar nebula of SN 1978K. At the distance of the host galaxy NGC 1313, 4.5 Mpc (de Vaucouleurs 1963), this upper limit on the size corresponds to 2.2 pc. This small size is more consistent with the sizes of LBV nebulae than WR nebulae, as also concluded by Chu et al. (1999).

In the case of SN 1998S, our observations cannot unambiguously determine whether the emission seen is circumstellar or interstellar. In either case, the nebular emission observed is no longer consistent with gas denser than the critical density needed for the auroral [N II] λ5575 line to dominate the nebular lines. Therefore, the density must be less than $\sim 10^5$ cm^{-3} and the emission seen is either from a lower density outer region of a circumstellar nebula or from interstellar material. If the narrow lines we detected are indeed circumstellar in origin, then the blueward velocity offset of the [N II] line relative to the Hα and [O III] lines may be caused by light travel time effects similar to those used to explain the early evolution of the [O III] line profile by Fassia et al. (2001).

Our high-dispersion (R$\sim$30,000) spectroscopic observations of SNe have demonstrated the possibility of detecting circumstellar nebulae ejected by SN progenitors and deriving information on the progenitors from the nebular properties. Our observations have also demonstrated the difficulty of such work because of the faintness of the SNe and their associated circumstellar nebulae. In order to identify emission from such nebulae, high-dispersion spectroscopic observations of SNe with large telescopes such as Gemini and Keck are needed. Only after a large number of such circumstellar nebulae have been detected and studied can we hope to better understand SN progenitors and their circumstellar environment.

We would like to thank the referee, E. Schlegel, for careful consideration of our original manuscript and insightful comments. In addition, we would like to thank P. Lundqvist for useful discussion of SN 1998S.

REFERENCES

Branch, D., & Cowan, J.J. 1985, ApJ, 297, L33

Burrows, C. J., et al. 1995, ApJ, 452, 680

[4]The theoretical PSFs were generated using Tiny Tim V5.0 written by John Krist and Richard Hook which is available from http://www.stsci.edu/software/tinytim.

Caraveo, P. A., Mignani, R., & Bignami, G. F. 1998, Mem. Soc. Astron. Italiana, 69, 1061

Chu, Y.-H., Caulet, A., Montes, M. J., Panagia, N., van Dyk, S. D., & Weiler, K. W. 1999, ApJ, 512, L51

Chu, Y.-H. 2001, in Young Supernova Remnants, AIP Conference Proceedings 565, eds. S. S. Holt and U. Hwang, 409

Chu, Y.-H., Weis, K., & Garnett, D. R. 1999, AJ, 117, 1433

Cowan, J.J., Henry, R.B.C., & Branch, D. 1988, ApJ, 329, 116

de Vaucouleurs, G. 1963, ApJ, 137, 720

Dunne, B. C., Gruendl, R. A., & Chu, Y.-H. 2000, AJ, 119, 1172

Fassia, A., et al. 2001, MNRAS, 325, 907

Fesen, R.A. 1985, ApJ, 297, L29

Filippenko, A. V. 1991, in SN 1987A and Other Supernovae, ed. I. J. Danziger & K. Kjär (Garching: ESO), 342

Filippenko, A. V., Barth, A. J., Bower, G. C., Ho, L. C., Stringfellow, G. S., Goodrich, R. W., & Porter, A. C. 1995, AJ, 110, 2261

Filippenko, A. V. 1997, ARA&A, 35, 309

Goodrich, R. W., Stringfellow, G. S., Penrod, G. D., & Filippenko, A. V. 1989, ApJ, 342, 908

Humphreys, R. M. & Davidson, K. 1994, PASP, 106, 1025

Hunter, D. A. & Gallagher, J. S. 1997, ApJ, 475, 65

Jha, S., Garnavich, P., Challis, P., & Kirshner, R. 1999, IAU Circ., 7107

Michael, E., et al. 2000, ApJ, 542, L53

Nicolaci da Costa, L., et al. 1998, AJ, 116, 1

Podsiadlowski, P. 1992, PASP, 104, 717

Points, S. D., Chu, Y.-H., Kim, S., Smith, R. C., Snowden, S. L., Brandner, W., & Gruendl, R. A. 1999, 518, 298

Salamanca, I., Cid-Fernanades, R., Tenorio-Tagle, G., Telles, E., Terlevich, R. J., Munoz-Tunon, C. 1998, MNRAS, 300, L17

Salamanca, I., Terlevich, R. J., & Tenorio-Tagle, G. 2002, MNRAS, in press

Schlegel, E. M. 1990, MNRAS, 244, 269

Smith, N., Humphreys, R. M., & Gehrz, R. D. 2001, PASP, 113, 692

Stathakis, R. A. & Sadler, E.M. 1991, MNRAS, 250, 786

Stockdale, C. J., Rupen, M. P., Cowan, J. J., Chu, Y.-H., & Jones, S. S. 2001, AJ, 122, 283

Tully, R. B. 1988, Nearby Galaxies Catalog, (Cambridge: Cambridge University Press)

Van Dyk, S. D., Hamuy, M., & Filippenko, A. V. 1996, AJ, 111, 2017

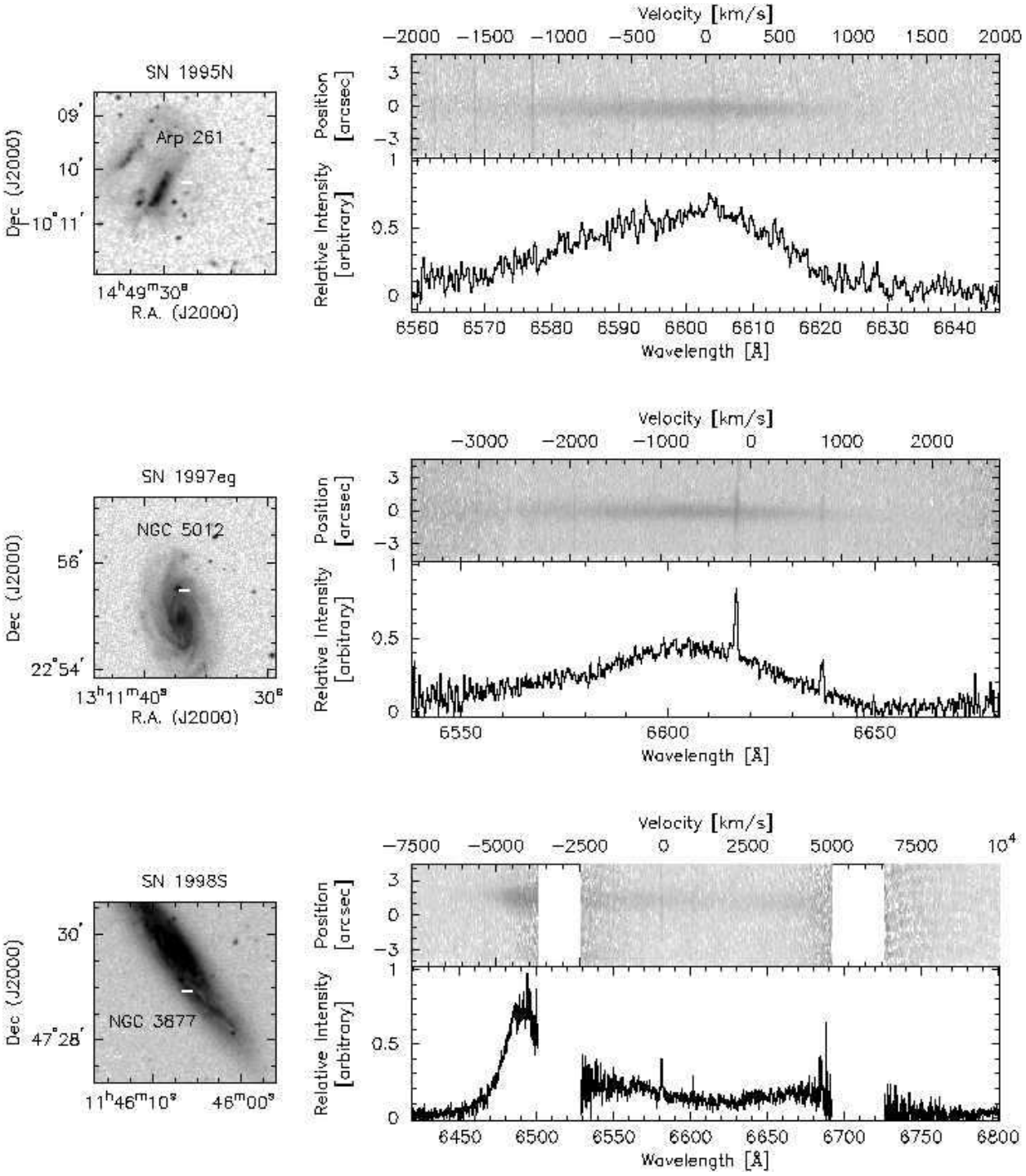

Fig. 1a.— Finding charts and Hα spectra of SN 1995N, SN 1997eg, and SN 1998S. (*Left column*) Digitized Sky Survey image of the host galaxy/environment for each SN. The slit position for the echelle observations is overlaid as a line segment. (*Right column*) The echellogram and the Hα line profile for each SN. The velocity scale at the top of each panel is relative to the systemic velocity of the galaxy. In some spectra gaps appear; these are cases where multiple echelle orders contain Hα emission from the SN ejecta.

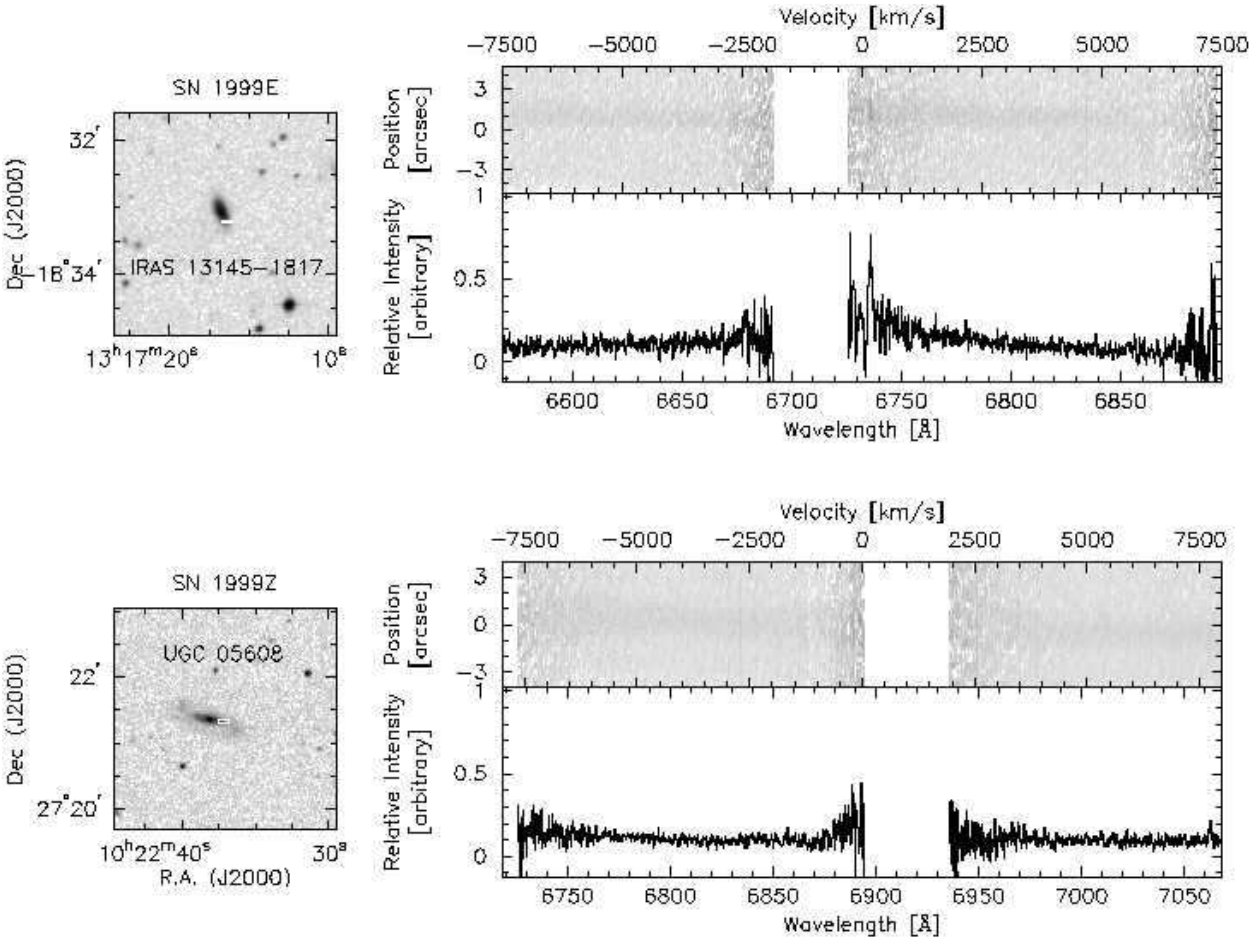

Fig. 1b.— Same as Figure 1a for SN 1999E and SN 1999Z.

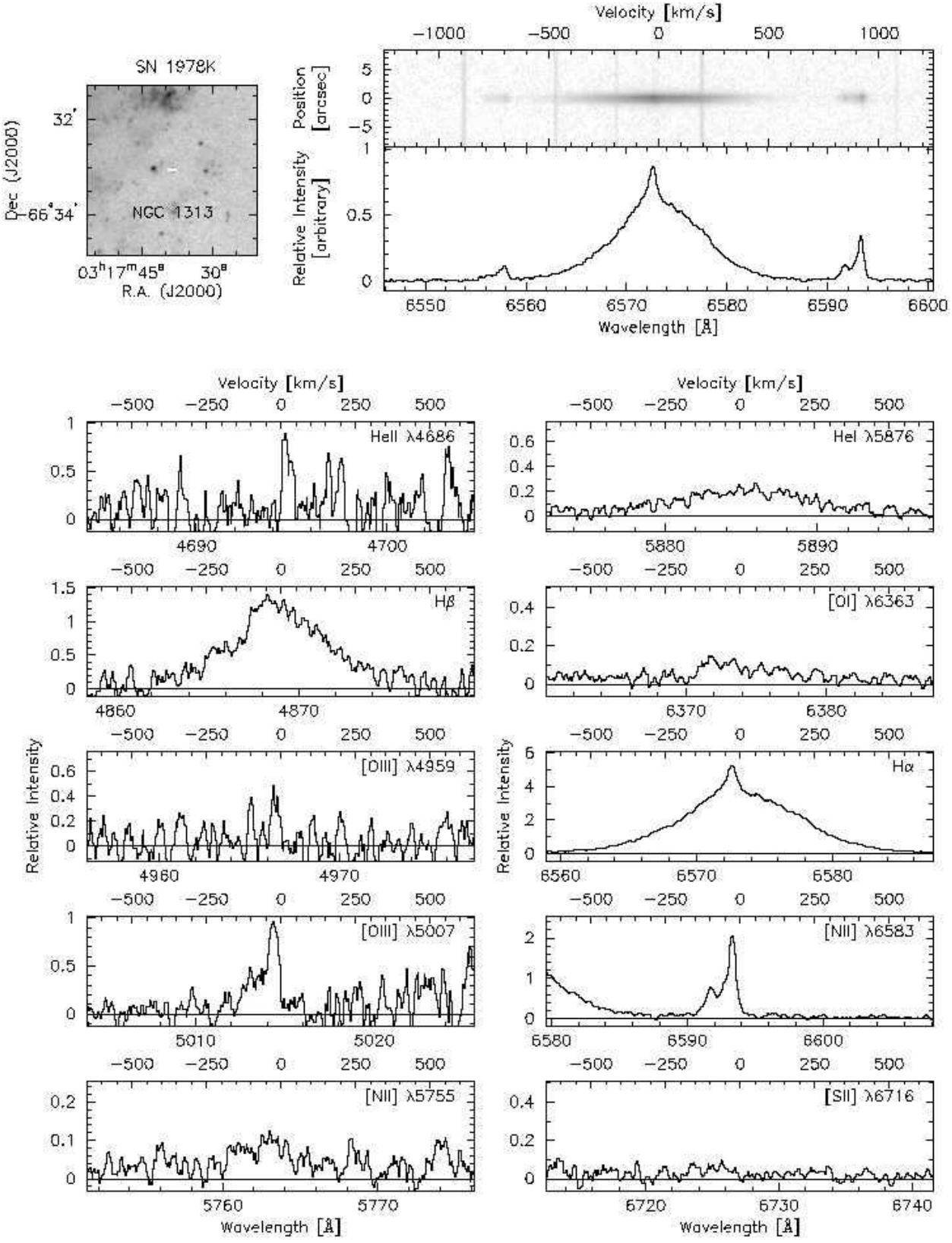

Fig. 2.— (*Top*) Same as Figure 1a for SN 1978K. (*Bottom*) Profiles of ten spectral lines from SN 1978K that were included in the echelle observations.

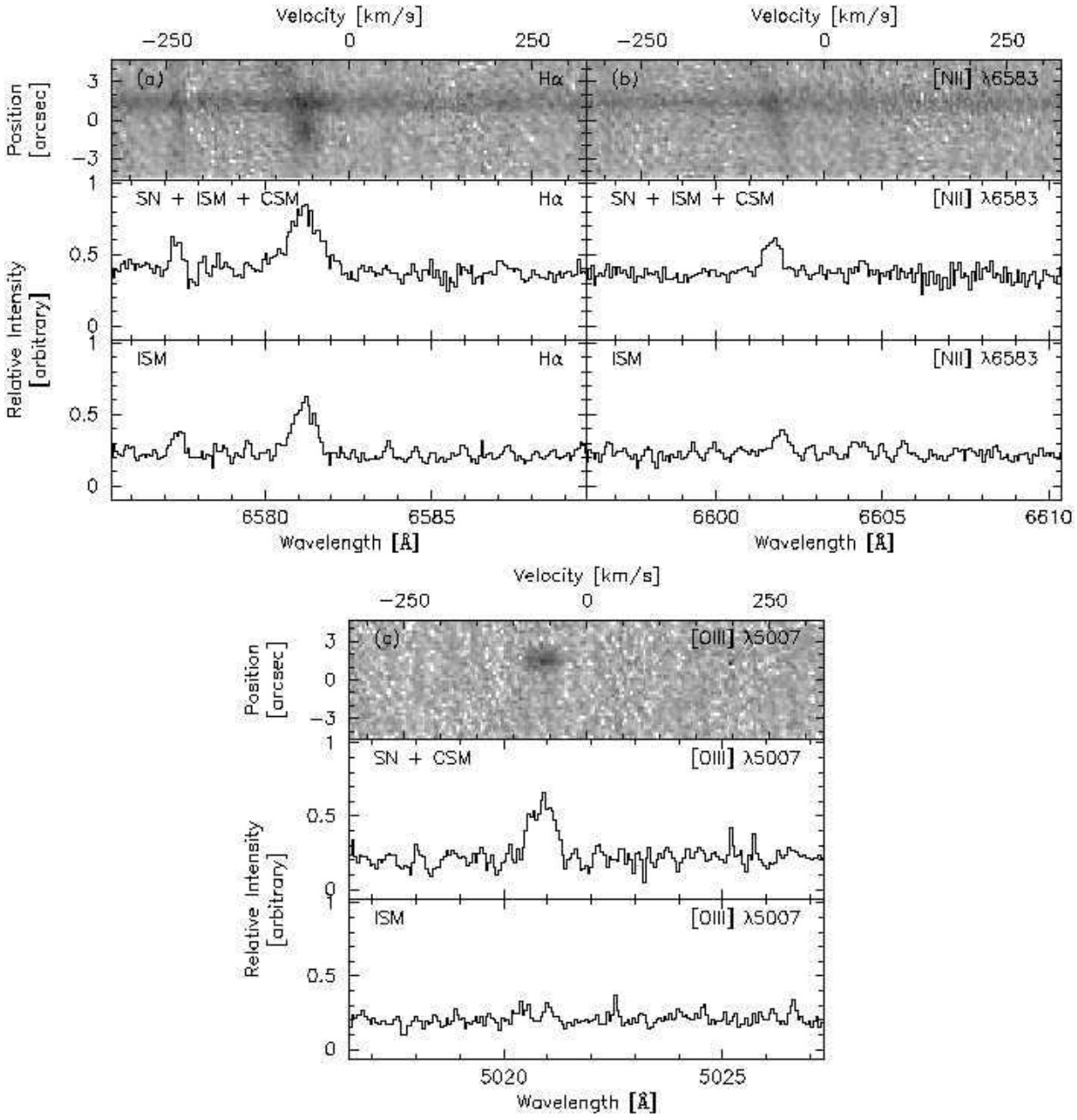

Fig. 3.— Narrow emission line components in the spectrum of SN 1998S near the systemic velocity of the host galaxy. (*Top left panel*) shows the Hα echellogram and the extracted spectrum on and off the SN. (*Top right panel*) shows similar details for the [N II] λ6583 line. (*Bottom panel* shows similar details for the [O III] λ5007 line.

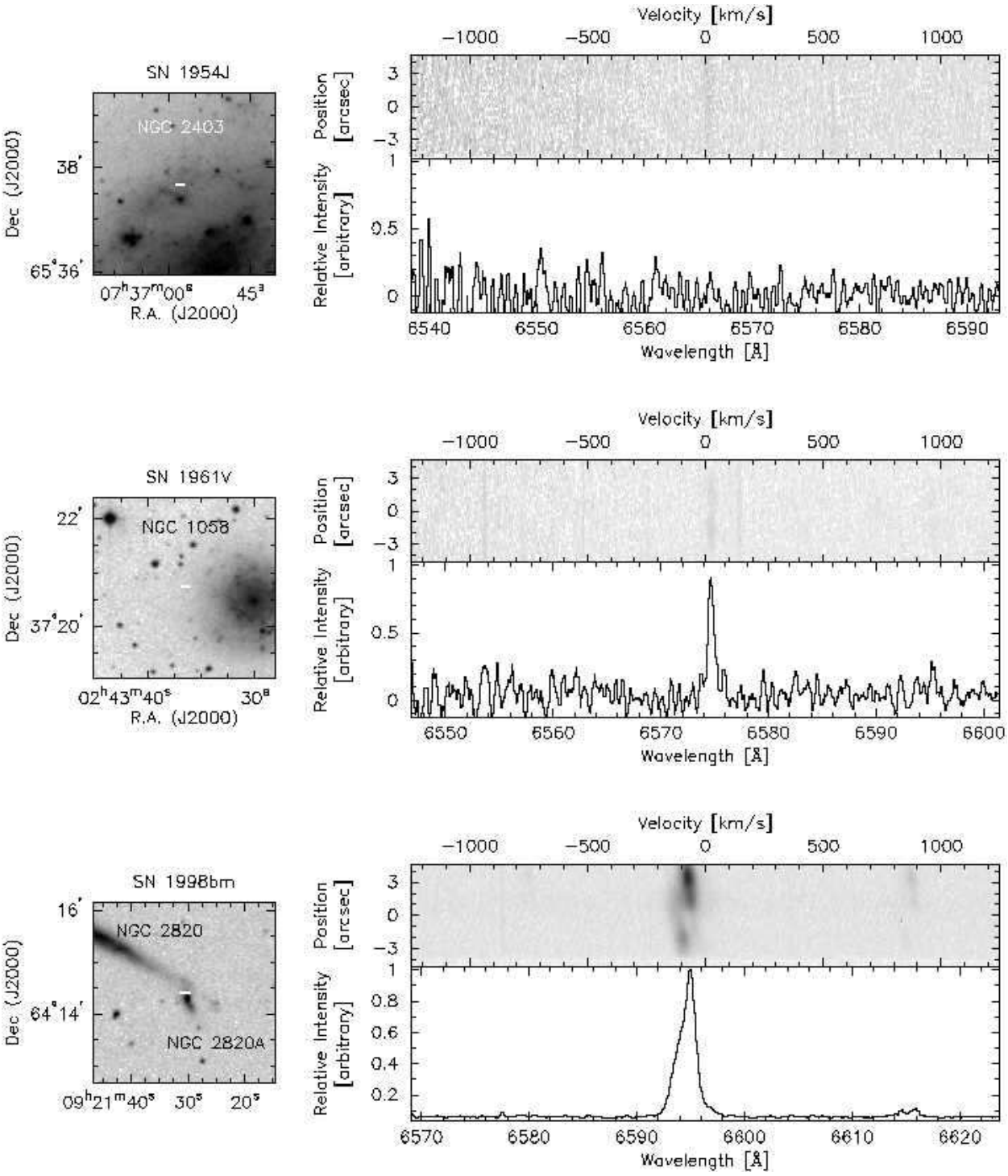

Fig. 4.— Same as Figure 1a for SN 1954J, SN 1961V, and SN 1998bm.

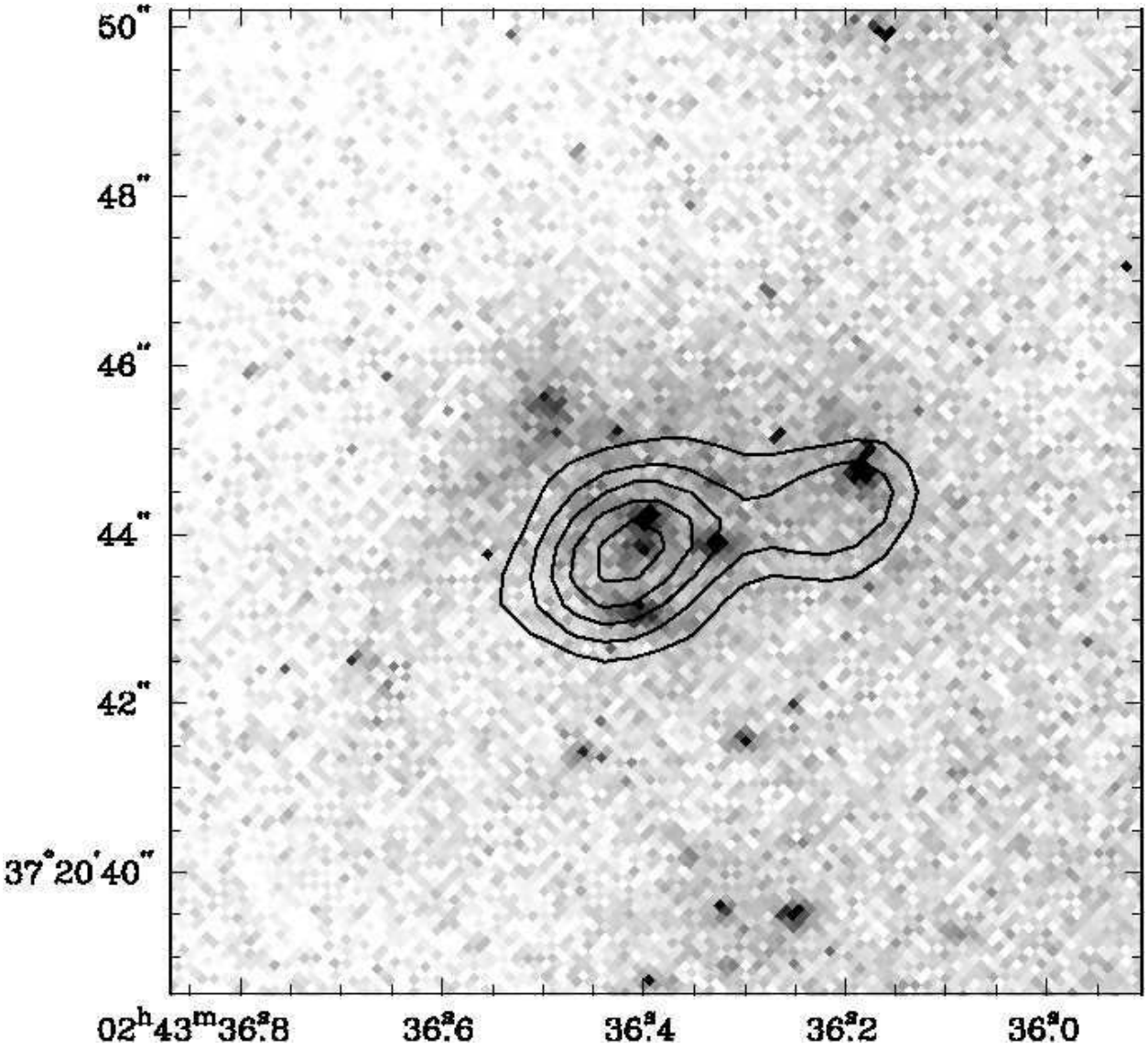

Fig. 5.— *HST* WFPC1 observations of SN 1961V with the F675W filter (greyscale image) overlaid with contours (0.07, 0.11, 0.15, 0.20, and 0.24 mJy) to show 6 cm radio continuum emission from the VLA observations by Stockdale et al. (2001). Coordinates given for the image are J2000. The radio continuum emission shows the two nonthermal radio sources while the *HST* shows the clusters in the centers of the two HII regions. Our echelle observations were centered on the HII region and thus may have missed the proposed optical counterpart for SN 1961V.

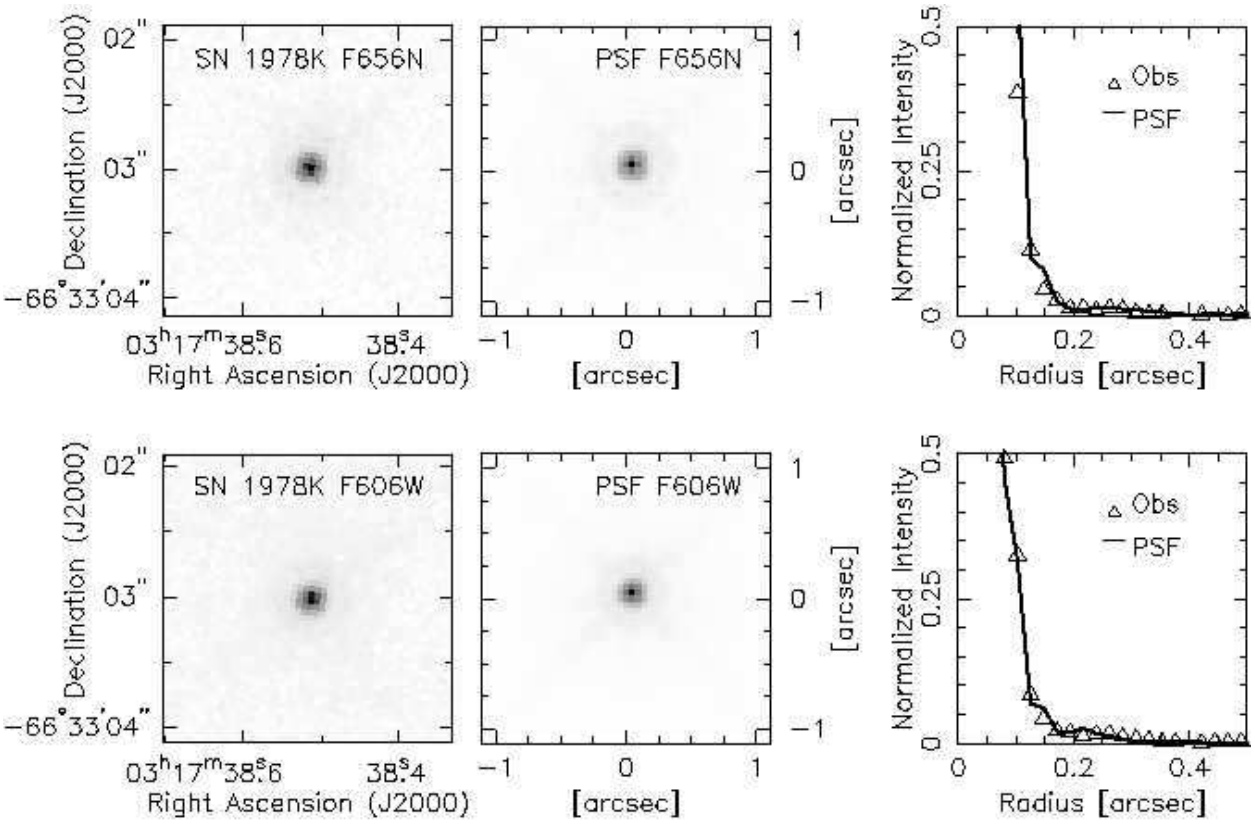

Fig. 6.— (*Top left panel*) *HST* Hα (F656N) image of SN 1978K, which was situated on the PC chip and is clearly unresolved. (*Top center panel*) Synthetic PSF generated by TinyTim, assuming a monochromatic point source, for comparison. (*Top right panel*) Average radial profile where the SN 1978K F656N observations are plotted using triangles and the PSF generated by TinyTim is shown as a solid line. (*Bottom left panel*) Broad-band (F606W) image of SN 1978K, also situated on the PC chip. Note the source size is indistinguishable from the narrow-band image. (*Bottom center panel*) Synthetic PSF generated by TinyTim for the F606W filter, using our echelle spectrum as input (i.e., no continuum emission). (*Bottom right panel)* Plot of average radial profile for the observations and synthetic PSF for the F606W observations (triangles) and model (solid line).

Table 1. Journal of Observations

Object	Date	Exposures[a]
SN 1954J	1999 Mar 3	1×1800
SN 1961V	1999 Mar 2	1×3600
	1999 Mar 3	2×1800
SN 1978K[b]	2000 Dec 5	3× 900
SN 1979C	1999 Mar 3	1×1800
SN 1992ad	1999 Mar 3	1×1800
SN 1993J	1999 Mar 2	1×1800
SN 1995N	1999 Mar 3	2×1800
SN 1996bu	1999 Mar 2	1×1800
SN 1997ab	1999 Mar 3	1×1800
SN 1997bs	1999 Mar 4	1×1800
SN 1997dn	1999 Mar 3	1×1800
SN 1997eg	1999 Mar 2	2×1800
SN 1998S	1999 Mar 2	1×1800
	1999 Mar 3	3×1800
SN 1998bm	1999 Mar 2	2×1800
SN 1999E	1999 Mar 3	1× 900
SN 1999Z	1999 Mar 4	2×1800

[a]Exposures are denoted as (number of exposures)× (exposure time in seconds for each exposure).

[b]Observations obtained with the CTIO 4m telescope (all other observations were obtained with the KPNO 4m telescope).

Table 2. Summary of Observations

Object	SN Type	Host Galaxy	Systemic Velocity[a] [km s^{-1}]	Hα Detected from SN	ISM	CSM
SN 1954J	IIpec	NGC 2403	131	no	yes	no
SN 1961V	IIpec	NGC 1058	518	no	yes	no
SN 1978K	IIpec	NGC 1313	475	yes	no	yes
SN 1979C	II-L	NGC 4321	1571	no	yes	no
SN 1992ad	II	NGC 4411b	1270	no	yes	no
SN 1993J	IIb	NGC 3031	−34	no	no	no
SN 1995N	II	Arp 261	1834	yes	yes	no
SN 1996bu	IIpec	NGC 3631	1156	no	no	no
SN 1997ab	IIn	HS 0948+2018	3598	no	no	no
SN 1997bs	IIpec	NGC 3627	727	no	yes	no
SN 1997dn	II	NGC 3451	1334	no	yes	no
SN 1997eg	IIpec	NGC 5012	2619	yes	yes	no
SN 1998S	II	NGC 3877	902	yes	yes	yes
SN 1998bm	II	NGC 2820/20A	1534/74	no	yes	no
SN 1999E	IIn	IRAS 13145−1817	7925[b]	likely	yes	no
SN 1999Z	IIn	UGC 05608	15453[b]	likely	yes[c]	no

[a]Systemic velocities of the host galaxies are given in the heliocentric frame and come from Tully (1988).

[b]The observed heliocentric velocity of the ISM component from this paper. These values are likely more accurate for the systemic velocity of the galaxy than previous values in the literature.

[c]The detection of emission from the ISM of UGC 05608 is based on Hβ, [S II], and [O III] emission but not Hα.